Ziegler-Nichols PID Controller Based Intelligent Fuzzy Control of a SPM System Design

JIUM-MING LIN and PO-KUANG CHANG
Ph.D. Program in Engineering Science, College of Engineering
Chung-Hua University
707, Sec. 2 Wu-Fu Rd. Hsin-Chu, 30012.
TAIWAN, R. O. C.
jmlin@chu.edu.tw http://www.cm.chu.edu.tw/chinese/teacher/MING/index.htm

Abstract: - This research is to use Ziegler-Nichols PID controller as a basement for the fuzzy controller design in the outer-loop of a Scanning Probe Microscope (SPM) to reduce the hysteresis effect. This improvement has been verified by practical implementation. Comparing the results with a previous design for the outer-loop with PI compensator, one can see that the proposed system is more robust.

Key-Words: - Ziegler-Nichols PID controller, PID Fuzzy controller, SPM, Hysteresis effect, LVT

1 Introduction

The SPM has been developed rapidly in last three decade [1]–[10]. Its usage is very extensive, e. g. the measurements of physical distribution and material property such as surface profile, roughness, static charge, magnetic dipole, friction, elasticity, and thermal conductivity. As the block diagrams in Fig. 1 of a previous research [11], a balance with stylus probe, force actuator, LVDT, load cell, personal computer, and XYZ-stages were integrated into a contact force-controlled SPM, such that the surface of the sample would not be destroyed by the stylus probe. To reduce the hysteresis effect of the force actuator this research in Fig. 2 applied a Ziegler-Nichols PID controller as a basement for the fuzzy controller design [12]–[15] in the outer-loop and LVT in the feedback loop of a SPM.

This improvement has been verified by practical implementation of a surface profiler. Comparing the results with the previous design for the outer-loop with PI compensator and inner-loop with Linear Velocity Transducer (LVT) for feedback, one can see that the proposed system is more robust.

The organization of this paper is as follows: the first section is introduction. The second and the third ones are respectively for the review of previous research and the proposed fuzzy controller design. The test results and discussions are given in Section 4. The last part is the conclusion.

2 Review of Previous System Design

The force actuator is consisted of a coil and a spring. As in Fig. 3(a) the rod returns to the initial place when the force actuator de-energized. On the other hand, if a voltage is applied across the coil, then there is current in the coil, and a force is generated to compress the spring and make the rod pull down as in Fig. 3(b).

The relationship of the applied voltage and displacement is shown in Fig. 4. To reduce the hysteresis effect of the force actuator in Fig. 4, this research is to use a fuzzy controller to replace the PI compensator for a previous research, the newly system model is shown in Fig.2. Table I listed the previous PI compensators [11] for inner and outer loops design (steady state errors are equal to zero for inner and outer loops) in Fig 1. In addition, the gain margins, phase margins of the inner (GM1, PM1) and outer (GM2, PM2) loops as well as the phase crossover frequency ω_c are also included.

Figs. 5-8 are the Bode plots of cases 1, 2, 5 and 6, respectively. The outputs of LVDT for saw tooth shaped input (as in Fig. 9) are shown from Figs. 10 to 13 for comparison (with hysteresis effect parameter H be 0.3). One can see that the larger the outer-loop phase margin, the lower the hysteresis effect, but all the hysteresis effects are still very dominant. The reason is ω_c are very large for these cases, and then the time and phase delays produced by the hysteresis effect would be increased. Thus the stability can even be degraded by adding the hysteresis effect to push the resulting phase margins be zero.

3 Ziegler-Nichols PID Controller Design

Ziegler and Nichols had proposed two famous PID controller design methods [12], which can be applied for a linear control system design. The details are briefed as follows.

3.1 Ziegler-Nichols PID Controller Design (Method 1)

The first one is applied for a system without the transfer function, one can make the unit-step input response as shown in Fig. 14, in which we can determine the gain K of the steady-state response, the time constant T, the y-intercept a of the intersect point of the maximum slope and the output axis as well as the time delay L. Then the transfer function of the plant is as follows:

$$G(s) = \frac{Ke^{-Ls}}{Ts+1} \quad (1)$$

The first PID coefficients selection rule is as listed in Table II, in which K_P, T_I and T_D are respectively the gain of PID controller coefficients and are related to the magnitudes of a and L. The abbreviation NA stands for not available.

Applying a unit step input to the previous system with PI compensator [11] for inner loop design (steady state error is equal to zero) in Fig 1, the unit step response is in Fig. 15. One can find that K=1, L=0.3, T=0.9 and a=0.25. By Table II one has the gains of PID compensator (1) as: K_P=4.8, T_I=0.6 and T_D=0.15. The response of the system with PID compensator (1) is in Fig. 16. One can see the performance of the result is better than those of the previous ones as in Fig.10-13 with D=0.3.

Table II The first Ziegler-Nichols PID coefficients selection rule.

Controller Type	K_P	T_I	T_D
P	$1/a$	NA	NA
PI	$0.9/a$	$3L$	NA
PID	$1.2/a$	$2L$	L/2

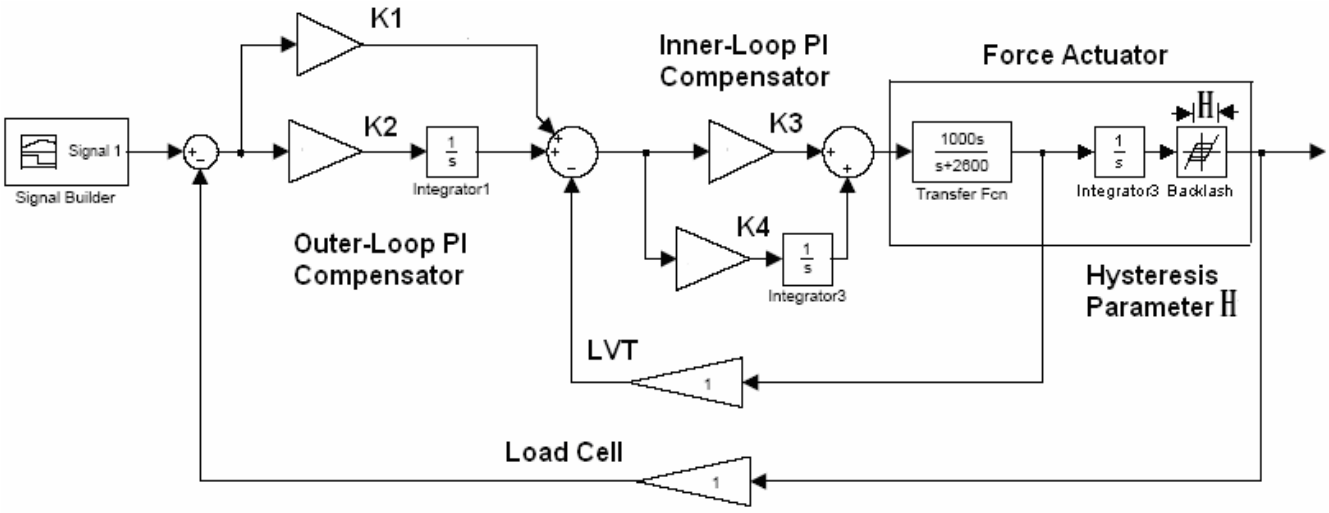

Fig. 1 Block diagram of SPM with LVT for inner-loop feedback in the previous research [11].

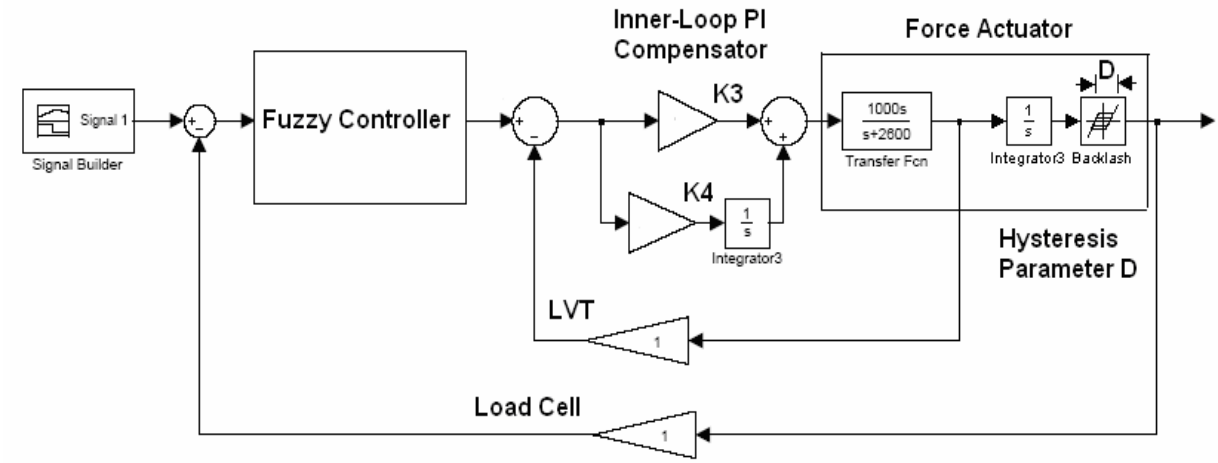

Fig. 2 Block diagram of SPM with a fuzzy controller in the outer-loop and LVT in the feedback loop of this research.

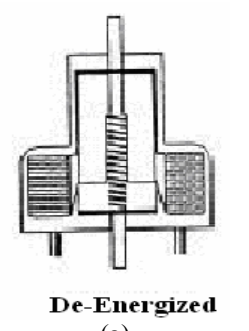

(a)

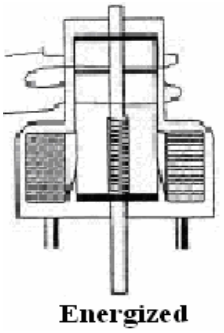

(b)

Fig. 3 Actuator operation states.

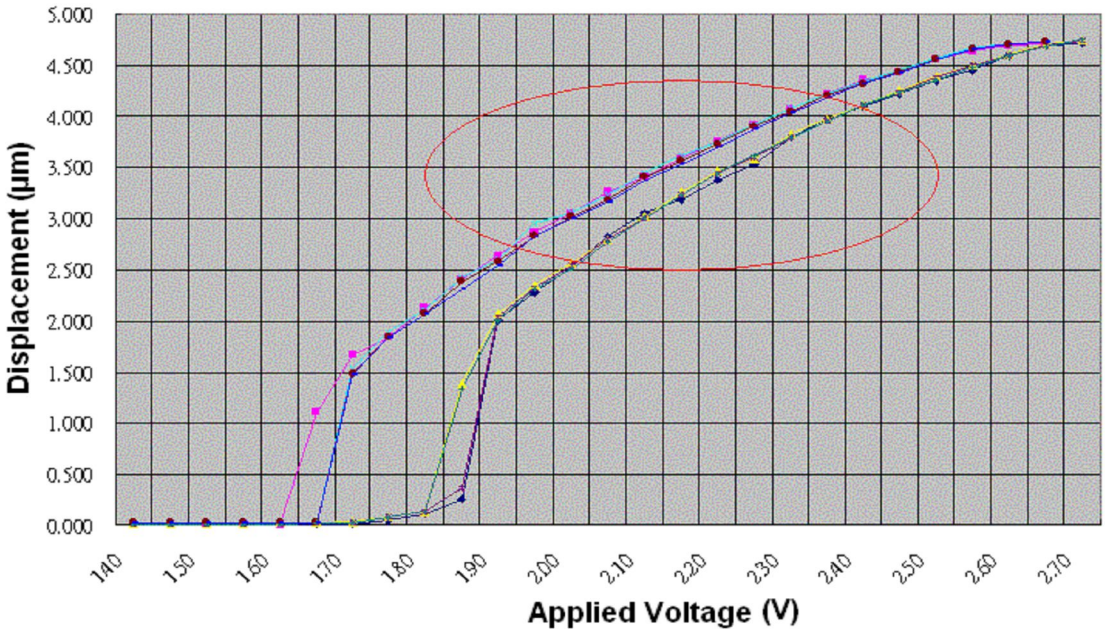

Fig. 4 Actuator applied voltage vs. displacement

Table I Previous design results of system in Fig. 1.

Case	K1	K2	K3	K4	GM1	PM1 (Deg)	GM2	PM2 (Deg)	ω_c (r/sec)
1	12	120	1	200	∞	73	∞	85	9840
2	10	100	0.8	180	∞	75	∞	70	7500
3	15	100	1.5	200	∞	65	∞	88	20000
4	20	150	2	150	∞	63	∞	89.5	40000
5	8	80	0.5	300	∞	85	∞	60	30000
6	18	200	1.3	220	∞	70	∞	90	30000

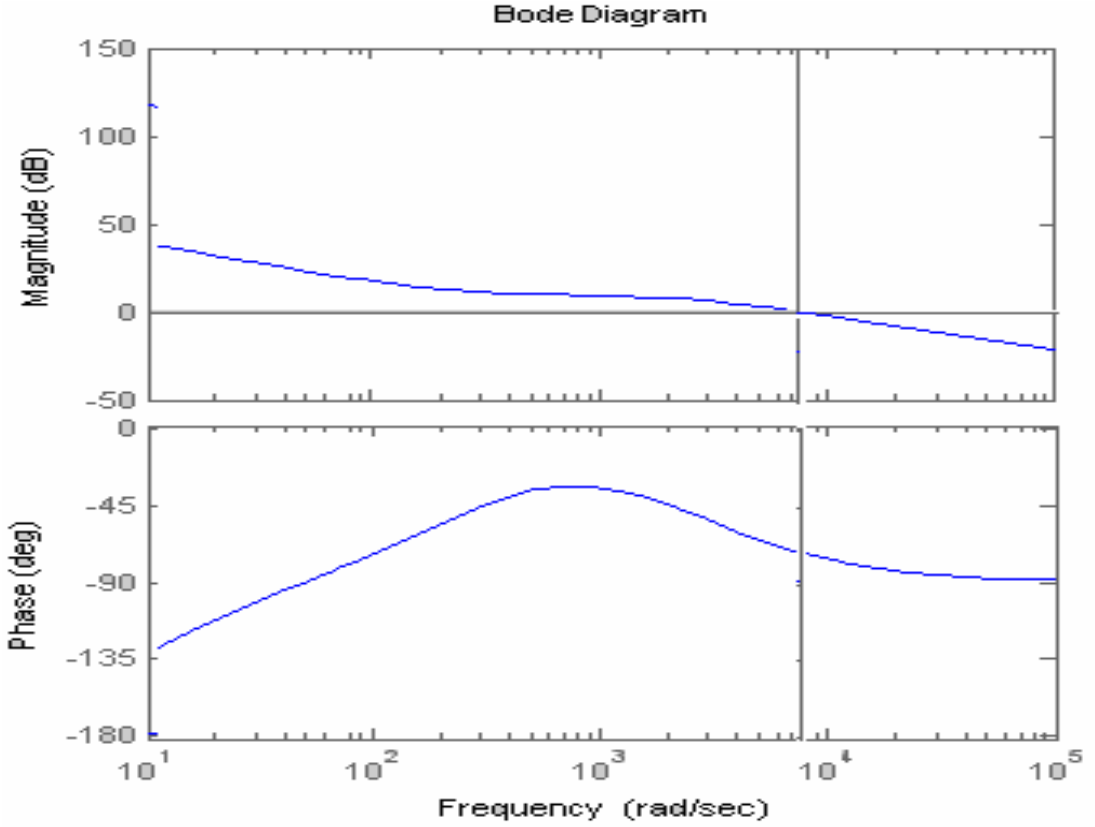

Fig. 5 Previous Bode plot of case 1 in Fig. 1.

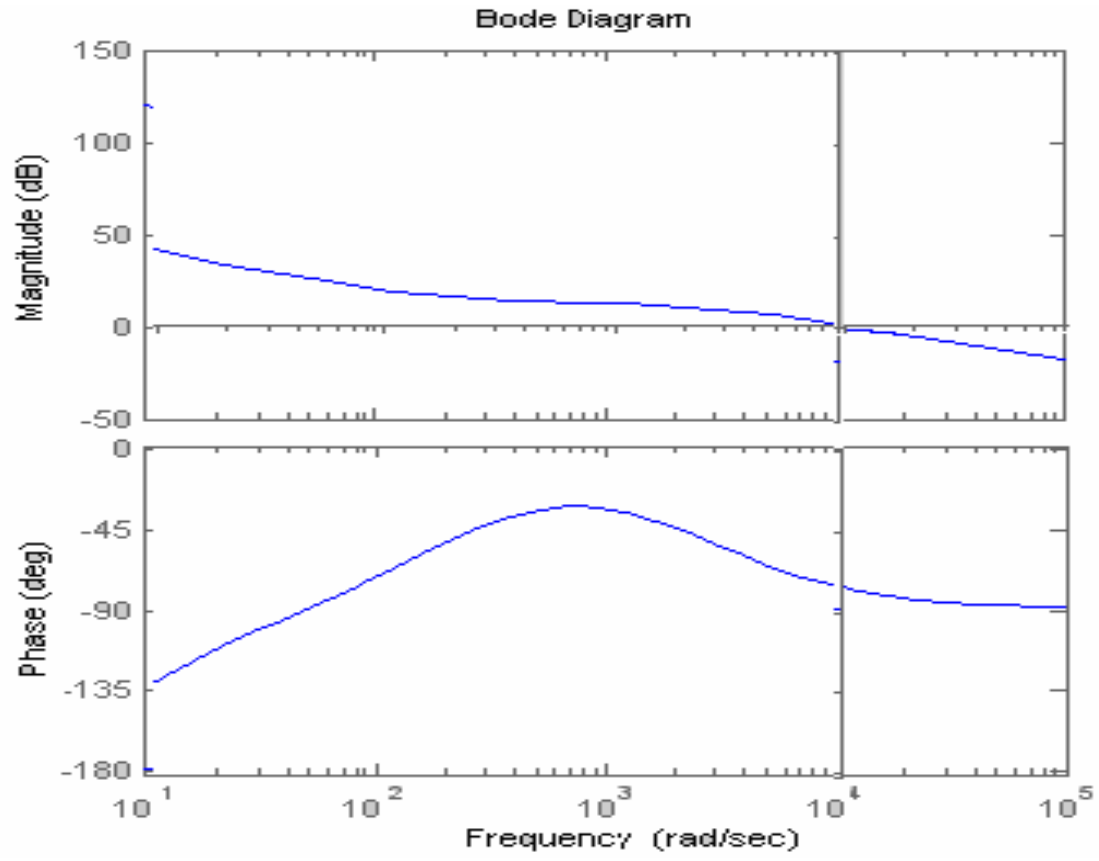

Fig. 6 Previous Bode plot of case 2 in Fig. 1.

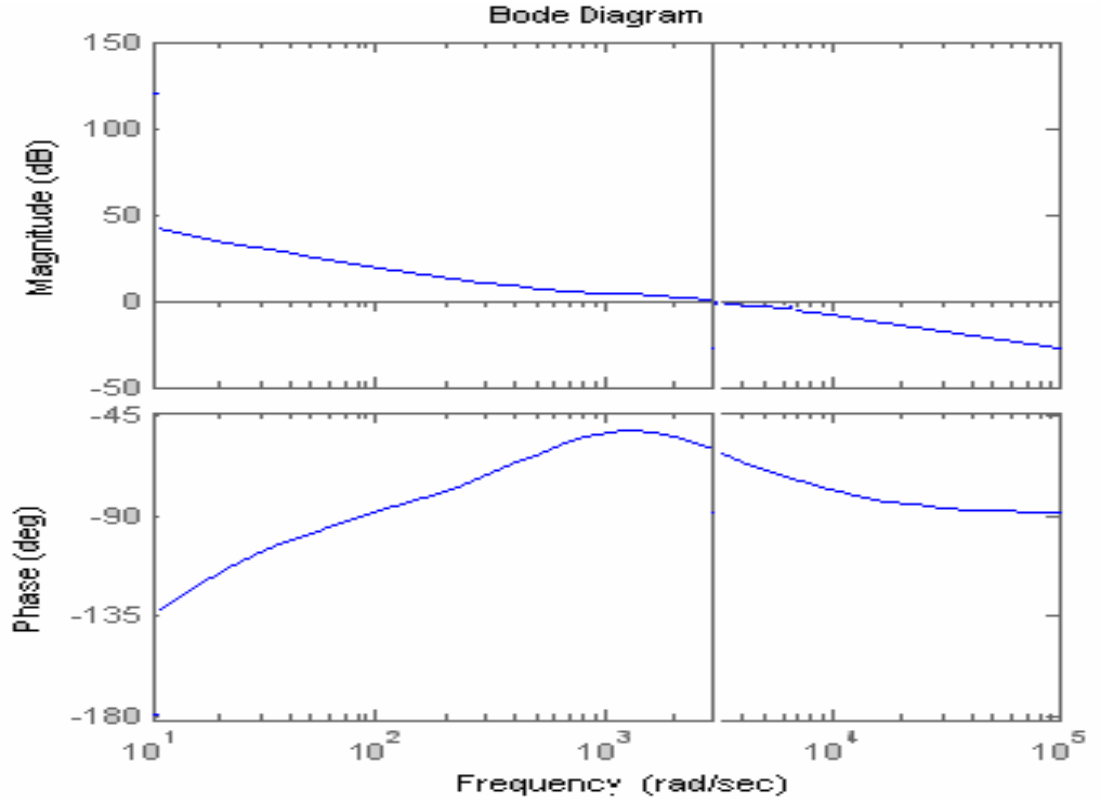

Fig. 7 Previous Bode plot of case 5 in Fig. 1.

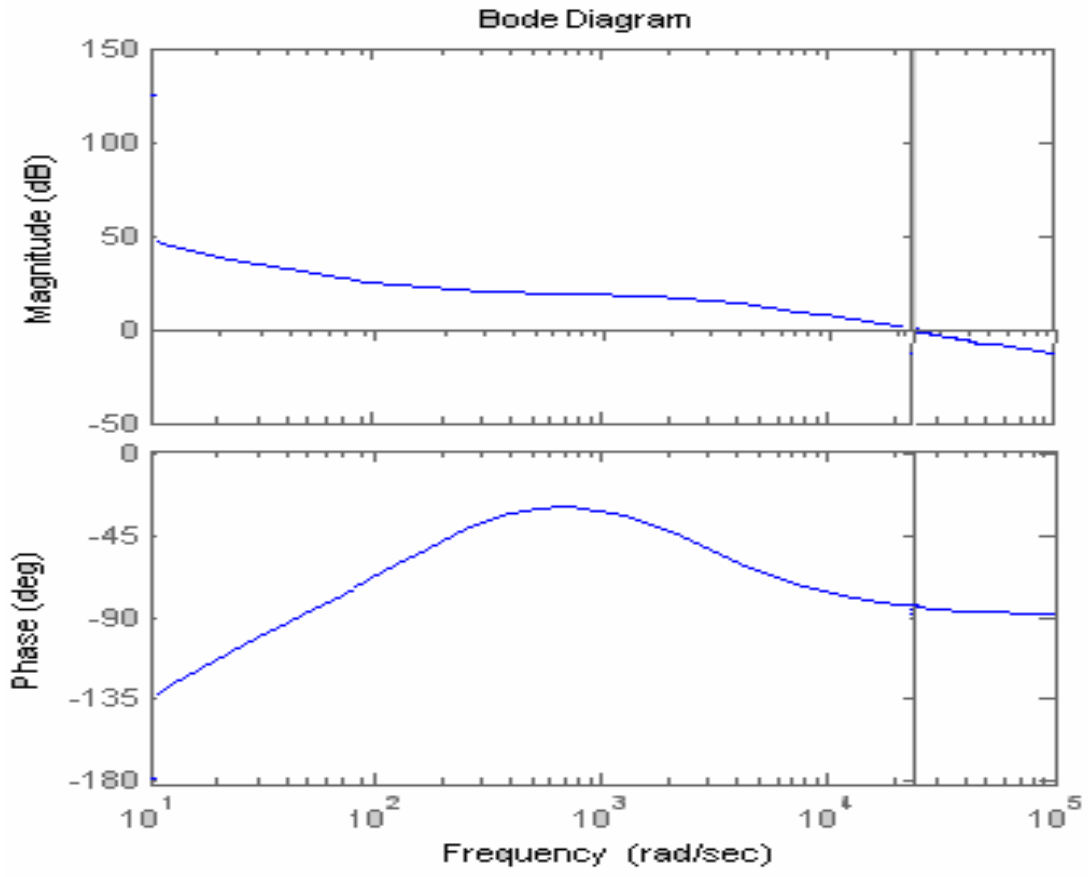

Fig. 8 Previous Bode plot of case 6 in Fig. 1.

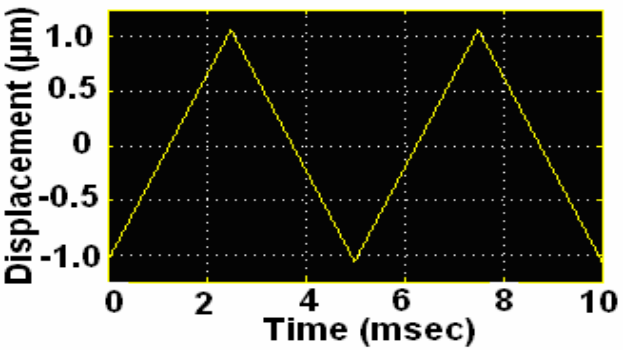

Fig. 9 A saw tooth shaped displacement command as input.

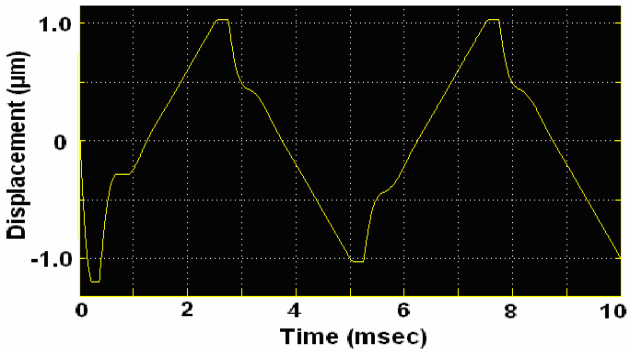

Fig. 12 Previous design output of case 5 in Fig. 1 (D=0.3).

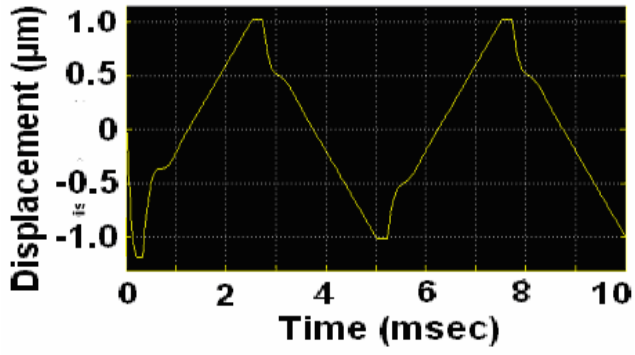

Fig. 10 Previous design output of case 1 in Fig. 1 (D=0.3).

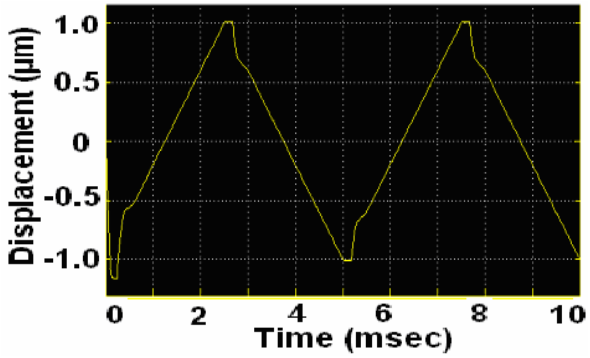

Fig. 13 Previous design output of case 6 in Fig. 1 (D=0.3).

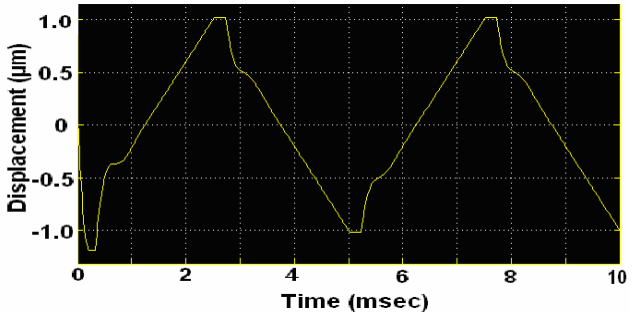

Fig. 11 Previous design output of case 2 in Fig. 1 (D=0.3).

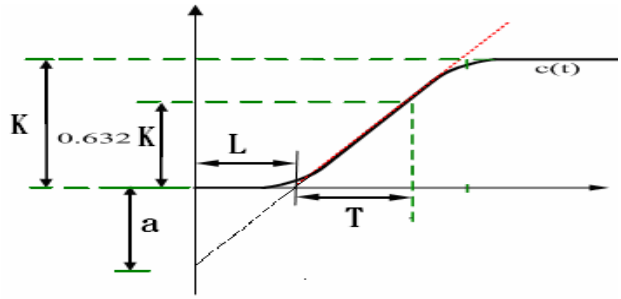

Fig. 14 The unit-step input response with a time delay.

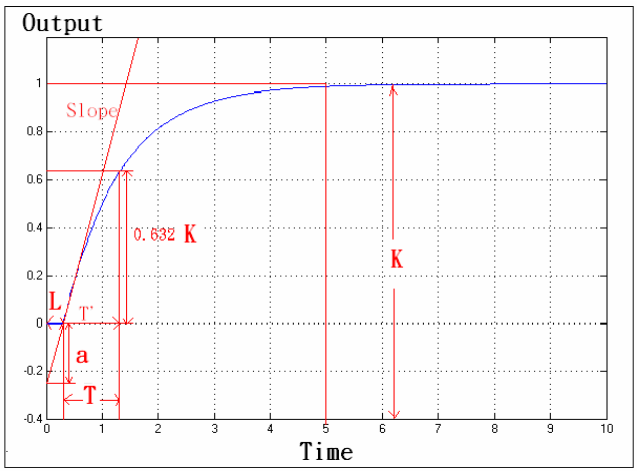

Fig. 15 The unit-step input response of a SPM system.

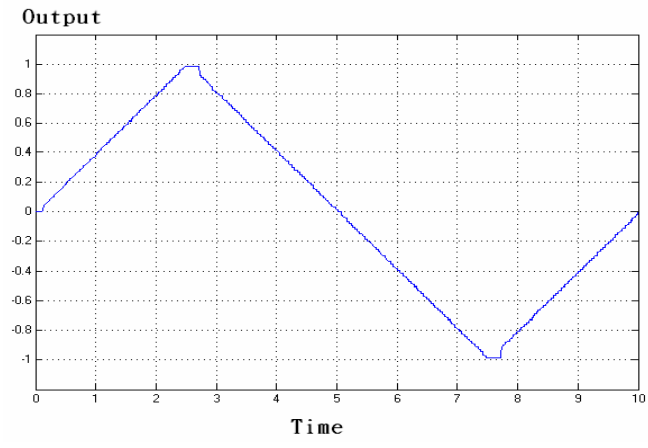

Fig. 16 The response of the system with Ziegler-Nichols PID compensator (1) and D=0.3

3.2 Ziegler-Nichols PID Controller Design (Method 2)

This method is applied for a system with a predetermined transfer function. Thus one can get the gain margin (GM) and the phase-crossover frequency ω from the Bode plot as in Fig. 17. Then one can obtain K_U and T_U as follows:

$$Ku = log^{-1}(\frac{GM}{20}) = 10^{\frac{GM}{20}} \quad (2)$$

and

$$Tu = \frac{2\pi}{\omega} \quad (3)$$

The second PID coefficients selection rule is as listed in Table III; one can see the gain of PID controller coefficients are related to the magnitudes of *Ku* and *Tu*.

Table III The second Ziegler-Nichols PID coefficients selection rule.

Controller Type	K_P	T_I	T_D
P	0.5*Ku*	NA	NA
PI	0.45 *Ku*	0.83*Tu*	NA
PID	0.6 *Ku*	0.5*Tu*	0.125Tu

The next step is to make the Bode plot of the previous system with PI compensator [11] for inner loop design (steady state error is equal to zero) in Fig 1, the result is as in Fig. 18. Thus one has GM=16.9dB and ω =7.7 rad/sec (phase-crossover frequency). The third step is to apply (2) and (3) to obtain *Ku*=7, and *Tu*=0.816. By Table III one has the gains of PID compensator (2) as: P=4.2, I=0.408 and D=0.102. The response of the system with PID compensator (2) is in Fig. 19. One can see the performance of the result is better than those of the previous ones as in Fig.10-13 with D=0.3.

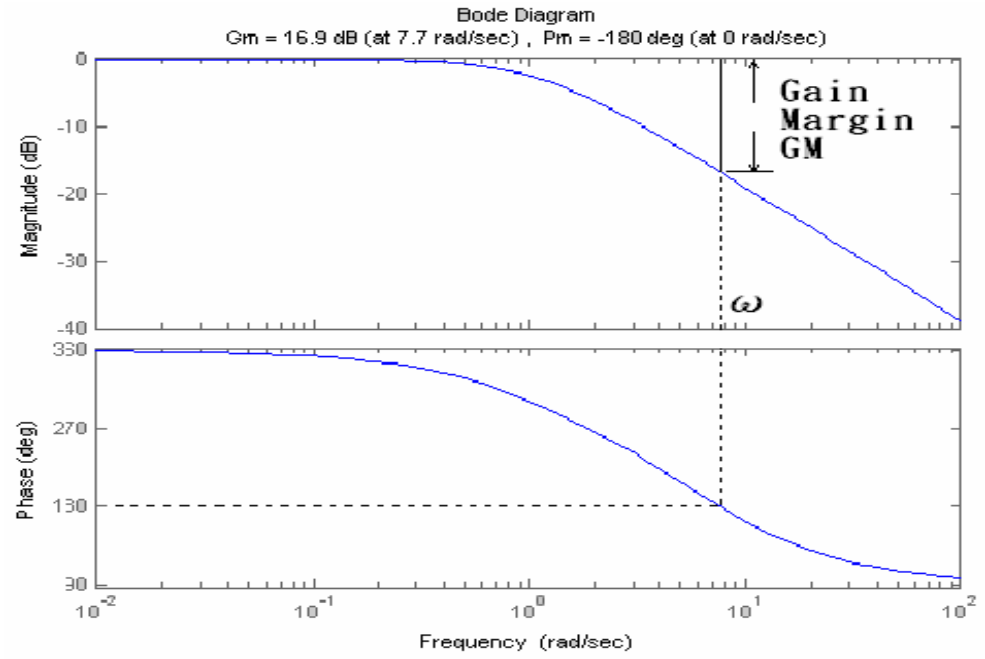

Fig. 17 The gain margin (GM) and the phase-crossover frequency ω of a control system defined in the Bode plot.

4 Fuzzy Controller Design

This section will directly apply the Ziegler-Nichols PID controller design results (Methods 1 and 2) obtained in Section III for the fuzzy PID controller design [12-15] as in Fig. 2. as shown in Fig. 20, which combines both an integrator and a fuzzy PD controller. It is well-known that fuzzy controller is based on the IF-THEN RULE as follows:

R1: IF E is NB AND ΔE is NB THEN U is NB,
R2: IF E is NB AND ΔE is ZE THEN U is NM,
R3: IF E is NB AND ΔE is PB THEN U is ZE,
R4: IF E is ZE AND ΔE is NB THEN U is NM,
R5: IF E is ZE AND ΔE is ZE THEN U is ZE,
R6: IF E is ZE AND ΔE is PB THEN U is PM,
R7: IF E is PB AND ΔE is NB THEN U is ZE,
R8: IF E is PB AND ΔE is ZE THEN U is PM,
R9: IF E is PB AND ΔE is PB THEN U is PB,

where NB, NM, NS, ZE, PS, PM, and PB respectively stand for negative big, negative middle, negative small, zero, positive small, positive middle and positive big.

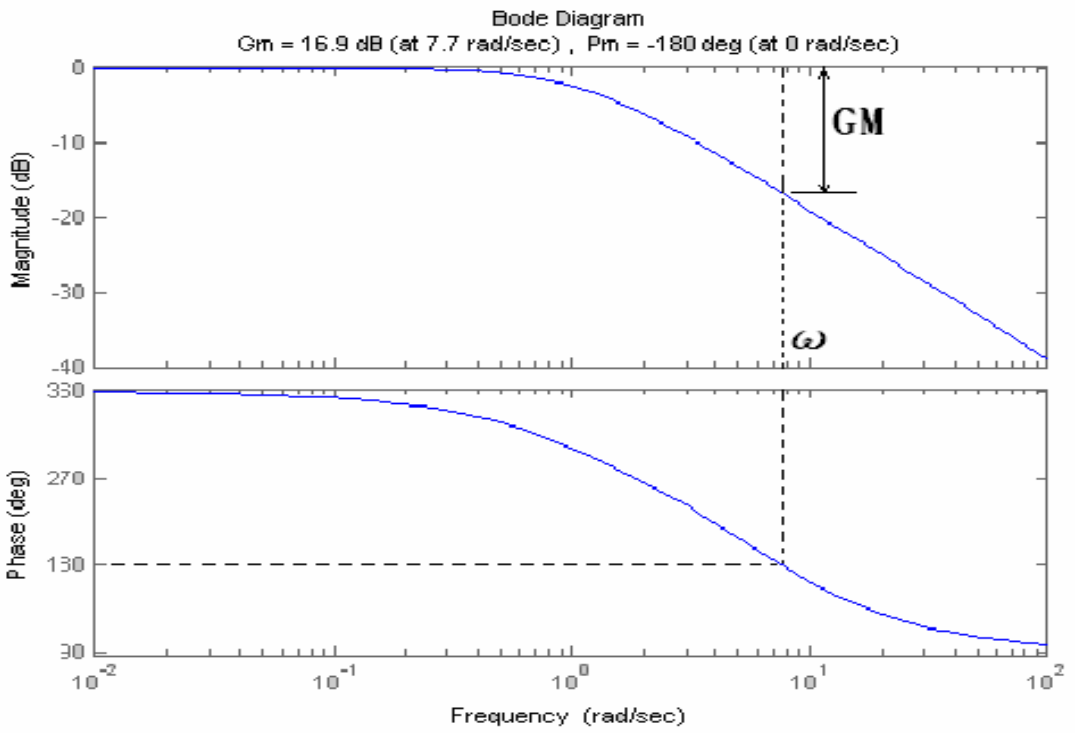

Fig. 18 The gain margin (GM) and the phase-crossover frequency ω of a SPM system defined in the Bode plot.

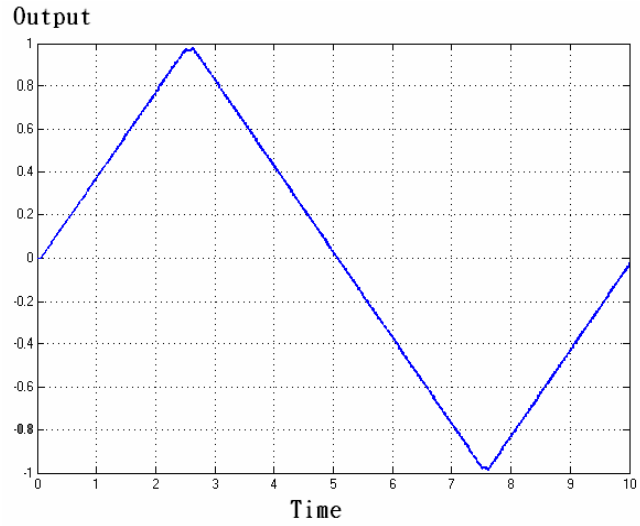

Fig. 19 The response of the system with PID compensator (2) and D=0.3.

The detailed cross reference rules for the inputs and output of fuzzy controller are defined in Table IV. According to fuzzy control design method the membership function parameters of error E, Δ E (deviations of present E and the previous E), and U (control input) are defined at first, which are listed in Table V. To reduce the computation time the triangular distribution functions are applied in fuzzy controller relationship functions calculation instead of using the traditional Gaussian ones.

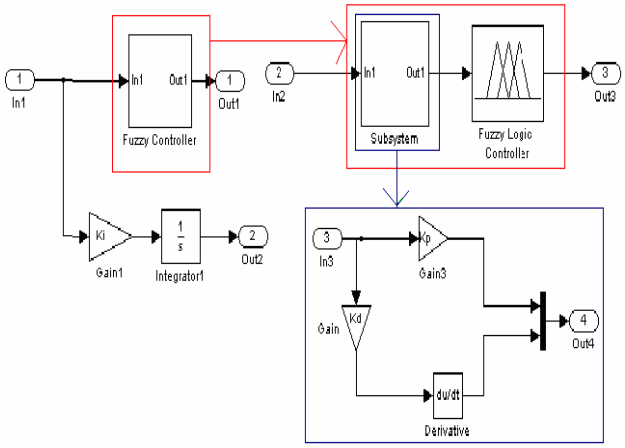

Fig. 20 The detailed structure of the fuzzy PID controller is obtained by applying an integrator and a fuzzy PD controller.

Table IV The detailed cross reference rules for the inputs and output of the fuzzy PD controller.

$E/\Delta E$	NB	NM	NS	ZE	PS	PM	PB
NB	NB	NB	NM	NM	NS	NS	ZE
NM	NB	NM	NM	NS	NS	ZE	PS
NS	NM	NM	NS	NS	ZE	PS	PS
ZE	NM	NS	NS	ZE	PS	PS	PM
PS	NS	NS	ZE	PS	PS	PM	PM
PM	NS	ZE	PS	PS	PM	PM	PB
PB	ZE	PS	PS	PM	PM	PB	PB

Table V. Fuzzy PD controller cross reference rules.

Item	Parameter E	Parameter ΔE	Parameter U
Negative Big (NB)	[-1 -1 -0.75 -0.3]	[-4.5 -4.5 -3.375 -1.35]	[-12 -12 -9.6 -8.4]
Negative Medium (NM)	[-0.75 -0.3 -0.15]	[-3.375 -1.35 -0.72]	[-9.6 -8.4 -7.2]
Negative Small (NS)	[-0.15 -0.1 0]	[-1 -0.5 0]	[-8.4 -4.8 0]
Zero (ZE)	[-0.05 0 0.05]	[-0.25 0 0.25]	[-4.8 0 4.8]
Positive Small (PS)	[0 0.1 0.15]	[0 0.5 1]	[0 4.8 8.4]
Positive Medium (PM)	[0.15 0.3 0.75]	[0.72 1.35 3.375]	[7.2 8.4 9.6]
Positive Big (PB)	[0.3 0.75 1 1]	[1.35 3.375 4.5 4.5]	[8.4 9.6 12 12]

4.1 Fuzzy Controller Design Based on Ziegler-Nichols PID Controller Design (Method1)

Fig. 21 shows the response of the system with fuzzy Ziegler-Nichols PID controller (1) (D=0.3). In addition, the XY-plot of input and output is as in Fig. 22. It can be seen that the hysteresis effect is almost disappeared, so that this method is better than those obtained by the previous PI controllers.

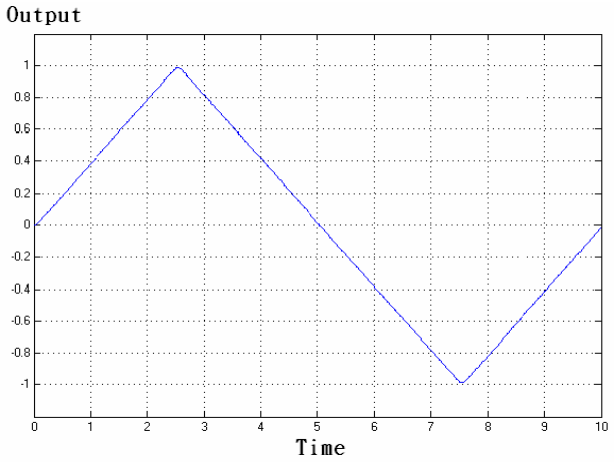

Fig. 21 The output response with fuzzy Ziegler-Nichols PID controller (1) (D=0.3).

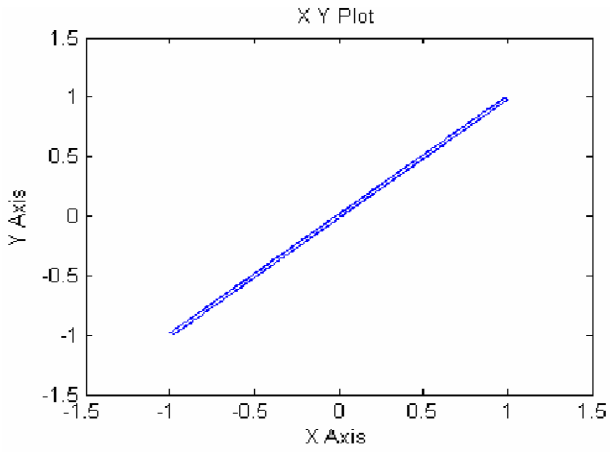

Fig. 22 The XY-plot of input and output for fuzzy Ziegler-Nichols controller (1) (D=0.3).

4.2 Fuzzy Controller Design Based on Ziegler-Nichols PID Controller Design (Method 2)

Fig. 23 shows the response of the system with fuzzy Ziegler-Nichols PID controller (2) (D=0.3). In addition, the XY-plot of input and output is as in Fig. 24. It can be seen that the hysteresis effect is almost disappeared, so that this method is better than those obtained by the previous PI controllers.

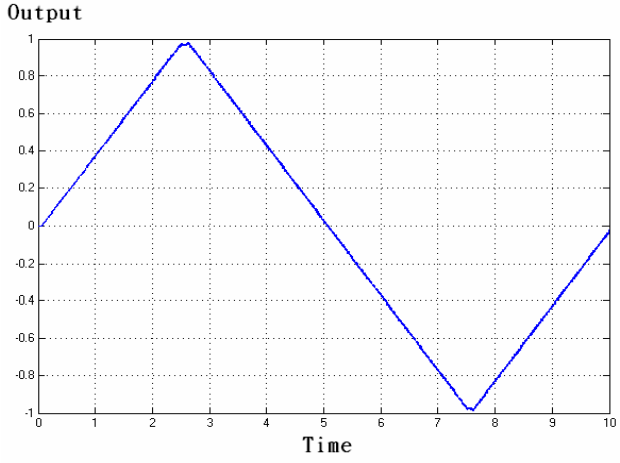

Fig. 23 The output response with fuzzy Ziegler-Nichols PID controller (2) (D=0.3).

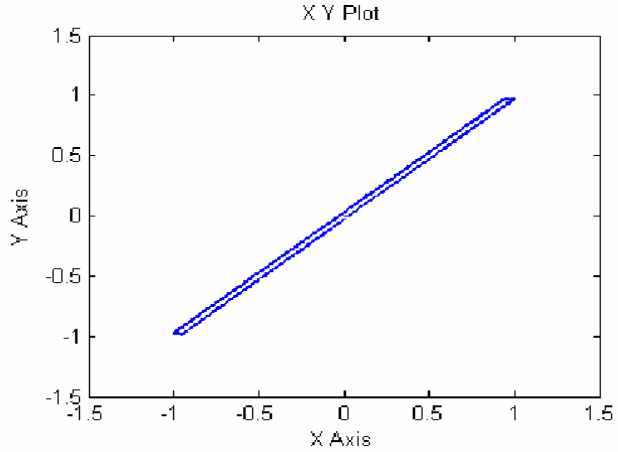

Fig. 24 The XY-plot of input and output for fuzzy Ziegler-Nichols controller (2) (D=0.3).

5 Test Results and Discussions

The operation steps are summarized as follows. The first step of test is initial leveling of the balance lever arm, which is achieved by adjusting the current through the coil of force actuator. Since the lever arm weight at the stylus probe (contact with the sample) side is heavier than the other side (contact with actuator) intentionally, thus the force actuator should push down to make the balance lever arm even. The contact point of the lever arm on the load cell is installed right at the calibrated-leveling height. This adjustment process stops when the value of load cell output increases from 0 mg to 40 mg. This value for the weight discrimination can be lowered if the circuit routing condition is better, thus the noise amplitude at the load cell output can be reduced.

The next step is to load the sample on the holder which is fixed on the piezo-stage as well as XYZ-stages, and then setting the XY-stages (the resolution is 34 nm in either axis) to make the first sampled point just right under the tip of the stylus probe, then raising the piezo-stage upward until the sampled point touching with the probe. The value of the probe contact force on the sample can be obtained by the load cell. In order to make sure that the probe contacts with the sample while not destroy it, the maximum contact force is limited to 100 mg, i.e., if the magnitude of contact force is smaller than 100 mg, then moving the piezo-stage upward by one step (the resolution is 10 nm), otherwise, stop. Then by scanning the XY-stages in either x- or y-axis, and finally, the surface profile of the sample obtained by the proposed fuzzy PID controller (1) can be obtained as shown in Figs.25 (a) and (b) for side view and top view, respectively.

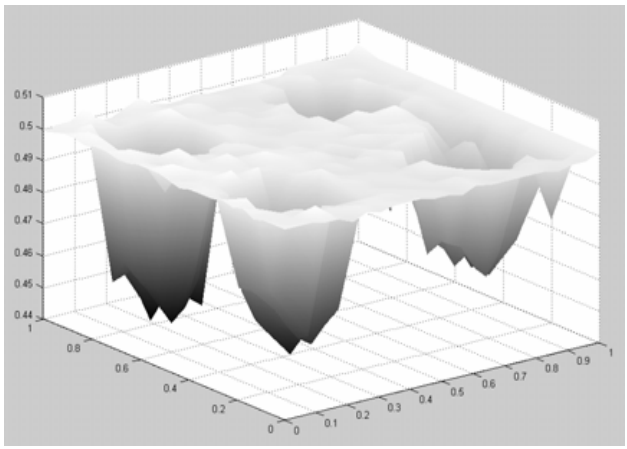

(a)Side view.

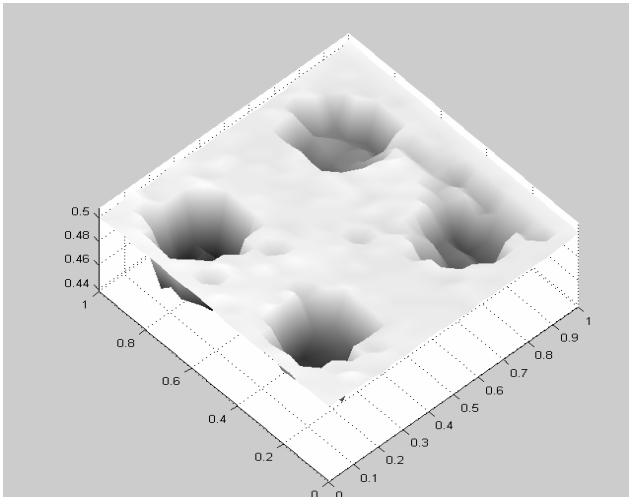

(b)Top view.

Fig.25 The surface profile of a sample with the proposed method

6 Conclusion

This research applied fuzzy Ziegler-Nichols PID control method for a Scanning Probe Microscope (SPM) system design. In addition, the actuator hysteresis effect was taken into consideration. Comparing the proposed method with a previous work are also made, it can be seen that the results of system performance obtained by the fuzzy Ziegler-Nichols PID controller (1) is much better. This improvement has been verified by MATLAB simulation and practical implementation of a surface profiler. Thus the proposed system is more robust. Finally, the profile of the object surface is displayed on a 3D graph.

Acknowledgment

This research was supported by National Science Council under the grants of NSC 95-2221-E-216-012, NSC 96-2221- E-216-029- and NSC 97-2221-E-216-013-MY2.

References:

[1] D. G. Chetwyud, , X. Liu and S. T. Smith, "A controlled-force stylus displacement probe," *Precision Engineering*, Vol. 19, October/ November 1996, pp. 105-111.

[2] X. Liu, D. G. Chetwyud, S. T. Smith, and W. Wang, "Improvement of the fidelity of surface measurement by active damping control," *Measurement Science Technology*, 1993, pp. 1330-1340.

[3] M. Bennett, and J. H. Dancy, "Stylus profiling instrument for measuring statistical properties of smooth optical surfaces," *Applied Optics*, Vol. 20, No.10, 1981, pp. 1785-1802.

[4] D. G. Chetwyud, X. Liu and S. T. Smith, "Signal fidelity and tracking force in stylus profilometry," *J. of Machinery Tools and Manufacture*, Vol. 32, No.1/2, 1992, pp. 239-245.

[5] G. Neubauer, "Force microscopy with a bidirectional capacitor sensor," *Rev. Science Instrument*, Vol. 61, 1990, pp. 2296-2308.

[6] M. Bennett, and J. H. Dancy, "Stylus profiling instrument for measuring statistical properties of smooth optical surfaces," *Applied Optics*, Vol. 20, 1981, pp. 1785-1802.

[7] J. I. Seeger, and S. B. Crary, "Stabilization of statistically actuated mechanical devices," *Electro-Transducers '97*, Chicago, IL, 1981, p. 1133.

[8] G. Haugstad, and R. R. Jones, "Mechanisms of dynamic force microscopy on polyvinyl alcohol: region-specific non-contact and intermittent contact regimes," *Ultra Microscopy*, Vol.76, 1999, pp.77-86.

[9] V. V. Prokhorov, and S. A. Saunin, "Probe-surface interaction mapping in amplitude modulation atomic force microscopy by integrating amplitude-distance and amplitude-frequency curves," *Appl. Phys. Lett.*, Vol. 91, 2007, pp. 1063-1065.

[10] J. M. Lin and C. C. Lin, "Profiler design with multi-sensor data fusion methods," *SICE Annual Conference 2007 in Takamatsu*, September 17-20, 2007, pp. 710-715.

[11] P. K. Chang and J. M. Lin, "Scanning probe microscope system design with linear velocity transducer for feedback compensation," *SICE Annual Conference 2008 in Tokyo*, August 20-22, 2008, pp. 2382-2387.

[12] H. Zhang and D. Liu, *Fuzzy Modelling & Fuzzy Control,* New York: Springer-Verlag, 2006.

[13] P. K. Chang and J. M. Lin, "Integrating traditional and fuzzy controllers for mobile satellite antenna tracking system design," *Proceedings of WSEAS Conference on Advances in Applied Mathematics, Systems, Communications and Computers,* selected papers from *Circuits, Systems and Signals 2008, Marathon Beach, Attica, Greece,* June 1-3, 2008, pp. 102-108.

[14] G. Bartolini, A. Ferrara, E. Usai, "Chattering avoidance by second-order sliding mode control," *IEEE Transactions on Automatic Control,* Vol. 43, February 1998, pp. 241-246.

[15] W. Perruquetti and J. P. Barbot, *Sliding Mode Control in Engineering*, CRC Press, 2002.